International Journal of Energy Research

INTERNATIONAL JOURNAL OF ENERGY RESEARCH
Int. J. Energy Res. (2016)
Published online in Wiley Online Library (wileyonlinelibrary.com). DOI: 10.1002/er.3536

A comprehensive stochastic energy management system in reconfigurable microgrids

Sajjad Golshannavaz[1,*,†], Saeed Afsharnia[2] and Pierluigi Siano[3]

[1]Electrical Engineering Department, Urmia University, Urmia, Iran
[2]School of Electrical and Computer Engineering, University of Tehran, Tehran, Iran
[3]Department of Industrial Engineering, University of Salerno, Fisciano, Italy

SUMMARY

This paper addresses the joint stochastic energy and reserve scheduling problem in microgrids (MGs). The established approach proposes a novel high-performance energy management system (EMS) making use of automatically controlled switches (ACSs). Accordingly, besides the optimal scheduling of active elements namely distributed generations (DGs) and responsive loads (RLs), the optimal topology of the network for each of the scheduling intervals is determined as well. Likewise, the effects of the reconfiguration process in probable variations of the scheduled energy patterns in DGs, RLs, and grid purchases are thoroughly assessed to highlight the alterations in unallocated capacities of these resources. Moreover, the uncertainties associated with both the load and wind speed forecasting errors are suitably accommodated through the reserve allocations. The proposed optimization procedure is formulated as a mixed-integer non-linear problem and resolved using a genetic algorithm (GA). The effectiveness of the projected framework is verified utilizing a typical MG, and the obtained numerical results are discussed in depth. Copyright © 2016 John Wiley & Sons, Ltd.

KEY WORDS

smart microgrids (MGs); optimal energy and reserve scheduling; distributed generation (DG); responsive load (RL); automatically controlled switch (ACS); reconfiguration

Correspondence

*Sajjad Golshannavaz, Electrical Engineering Department, Urmia University, Urmia 5756151818, Iran.
†E-mail: s.golshannavaz@urmia.ac.ir

Received 15 December 2015; Revised 11 February 2016; Accepted 4 March 2016

1. INTRODUCTION

Being justified by the impressive technical and economical merits, the integration of distributed energy resources (DERs) in low voltage distribution networks is well-recognized as a persuasive and practical remedy for accommodating the electrical energy requirements of societies. Today, besides the conventional diesel-based distributed generations (DGs), renewable energy resources such as wind turbines (WTs) or solar panels represent an important opportunity to enrich the modern electrification networks with clean energies [1]. In this theme, some supporting technologies including complex operational strategies, based on reserve scheduling, have been suggested by some researchers in order to cope with the intermittent nature of these resources [2].

Meanwhile, in order to assure a sustainable future for the energy sector, electric power regulators have motivated the utilities to effectively restructure themselves [3]. Being biased with the recent advances in information and communication technology (ICT) along with the prompt growth of infield intelligent electronic devices (IEDs), the notion of smart grid has evolved in power systems and specifically at the distribution level. Aligned with the technical features, more intelligent application systems with online control capabilities are now restructuring the existing passive structures into active networks where the 'connect and forget strategy' is gradually given up [4]. As one of the leading categories of smart grids, medium voltage, or low voltage microgrids (MGs) are hosting several active elements. Embedded generations such as dispatchable diesel-based DGs or non-dispatchable renewable-based DGs, active consumers, demand side management programs including responsive loads (RLs), and automatically controlled switches (ACSs) are some of the main ingredients of MGs [5]. Considering all the aforementioned elements, the operational scheduling of a MG in different time horizons is now a challenging task which necessitates the development of efficient energy management systems (EMSs). The EMS represents the central core of technical and economical optimizations in MGs. By collaborating with a well-structured data acquisition system and utilizing optimal load flow algorithms, the EMS determines the optimal scheduling decisions of all active elements as well as MG's optimal energy transfer with the upstream network. The operational planning of a MG is in essence an internal operational decision making tool and the MG operator (MGO) tackles it through the established EMS. With higher levels of uncertainties associated with the renewable energy resources as well as load variations, the scheduling approach should determine the optimal amounts of reserve quantities to be dispatched in real-time horizons. It is worthy to note that the MGO benefits the unallocated capacities of its internal resources to provide the required reserve quantities. However, the provided energy and reserve requirements through the upstream grid are transferred as the participation bids for distribution system operator to be cleared in an internal distribution market [6,7].

As clarified, devising a comprehensive EMS is required to guarantee the successful performance of MGs [8–13]. In this context, the daily operational scheduling of MG has gained more attention in recent years. In [14] the authors have contributed by proposing an innovative EMS for daily operational planning of DGs and WTs. Also, some other studies such as [15,16] have surveyed the participation of MGs with demand side management programs. The existing challenges along with the possible achievements and the promising merits of RLs are underlined by these studies in conjunction with operational scheduling of the network activities. Moreover, some of the EMS algorithms have also paid attention to the technical aspects such as voltage control processes. In this way, authors in [17] have established an efficient EMS algorithm to regulate the DG power factor along with other elements of the MG. Furthermore, the scheduling time horizon is made shorter by proposing a two-stage EMS framework in [18]. In this study, the first stage performs a daily scheduling of resources whereas the effect of real-time data is subsequently explored in the second stage. Observing the uncertainties in load forecast and wind speed prediction errors, authors in [19,20] have explored the simultaneous energy and reserve dispatching of DGs and RLs. They have developed efficient EMS models in which the existing uncertainties in MG's load and wind speed variations are rehabilitated by devoting adequate reserve quantities. What is more, the available ACSs in smart MGs require deeper research studies to guarantee their successful deployment. Although, there have been remarkable efforts in networks' topological reconfigurations, these surveys have merely dealt with long-term periods [21–23]. The voltage profile improvement and power losses reduction are the two most important objectives in such studies. In spite of this, it is now a sensible fact that the daily reconfigurations through ACSs could bring further technical and monetary savings for utilities and MGs. Although the investigated literatures have presented forward steps in fulfillment of EMS capabilities, this research topic is still worth of investigation.

In brief, the main innovative contributions of the proposed article can be listed as follows:

- Devising an efficient EMS for optimal daily operational scheduling of emergent MGs;
- Simultaneous joint stochastic energy and reserve scheduling of a MG for suitable accommodation of uncertainties;
- Incorporating short-term flexible network reconfigurations through ACSs to enhance the techno-economical performance of a MG;
- Considering practical switching limitations and costs of ACSs to achieve a practical EMS scheme;
- Proposing the utilization of unallocated capacities released by hourly reconfigurations of the MG as reserve capacities.

As an innovative contribution, deployment of ACSs makes MGO capable of remotely reconfiguring the network's topology in order to attain different objectives. Consequently, besides the optimal control of active elements including DGs and RLs, the optimal topology of the network for each of the scheduling intervals is determined as well. Furthermore, the proposed framework embraces the maximum switching operations limit and switching costs of ACSs to guarantee their acceptable life-time. As well, the load and wind speed prediction errors are well-regarded in EMS design through a scenario-based reserve allocation approach. Hence, besides the optimal energy dispatching of active elements, the effect of topological variations in capacity release of all MG's resources is deeply assessed. The unallocated capacities could be hence envisaged as reserve resources to alleviate the concerns associated with uncertainties. Thus, an optimal reserve scheduling process is devised to lessen the expected demand not supplied (EDNS) index and hence increasing the load serving reliability. Further discussions are also provided to highlight the possible improvements through the proposed EMS design.

The remainder of this paper is organized as follows. Section 2 addresses the generic description of the proposed intelligent data acquisition system and EMS framework. Section 3 formulates the proposed joint stochastic energy and reserve scheduling approach. Section 4 interrogates several test cases and provides numerical results. Eventually, the concluding remarks are provided in Section 5.

2. STRUCTURE OF THE PROPOSED INTELLIGENT DATA ACQUISITION SYSTEM AND EMS ARCHITECTURE

2.1. MG intelligent data acquisition system

Figure 1 demonstrates the structure of the proposed intelligent data acquisition system. Besides connecting to the upstream grid, the MG also encompasses DGs, WTs, RLs, and ACSs as active elements. Also, different sorts of

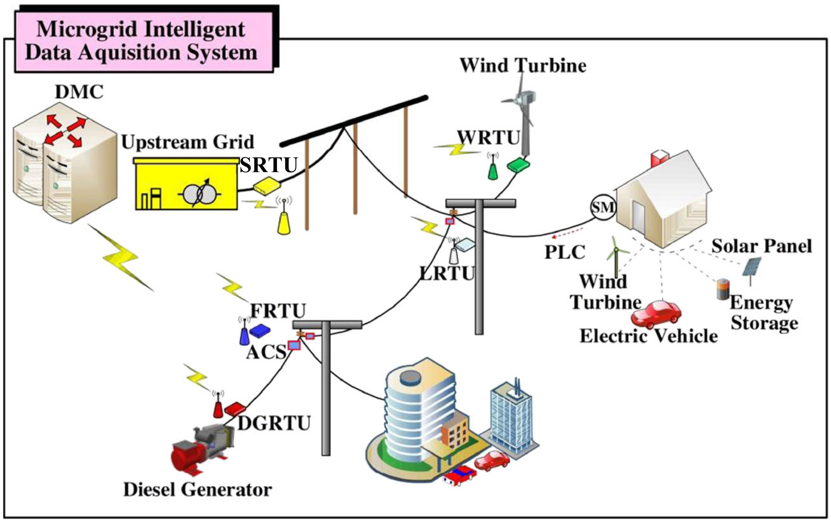

Figure 1. Schematic representation of the MG's intelligent data acquisition system.

remote terminal units (RTUs), serving as infield IEDs, are installed. In the residential areas, by utilizing power line carrier (PLC), smart meters (SMs) are sending the end-side data to a higher level namely load RTUs (LRTUs). LRTUs are communicating with a data management center (DMC) based on wireless general packet radio service (GPRS) to deliver the aggregated data. It is worth noting that the same path is deployed to transfer the MGO signals to the end-side consumers as well. Considering different types of DGs, they are endowed with distributed generation RTUs (DGRTUs) in order to effectively cooperate with the DMC. Low voltage feeder RTUs (FRTUs) are endowed with ACSs enabling the MGO to wisely consider topological reconfigurations in scheduling process of the MG. Likewise, FRTUs are equipped with strong bidirectional protection schemes in order to ensure a safe operational strategy. A substation RTU (SRTU) is also available to provide proper control on substation apparatus and the external grid activities. Eventually, the DMC delivers the total data and the network status to be taken in use by the EMS.

2.2. Architecture of the proposed EMS

The illustrative architecture of the proposed EMS, as a set of hardware/software system applications, is depicted in Figure 2. The EMS is fed by a DMC data regarding all its network components. The latest state of the ACSs and of the network topology is made available through the communication system by the DMC. Besides, a strong database including MG's network model and associated information is intended as one of the fundamentals of the EMS. Natural resources, such as wind speed or solar radiation as well as network's load demand, are forecasted utilizing high-performance forecasting algorithms. Also, the

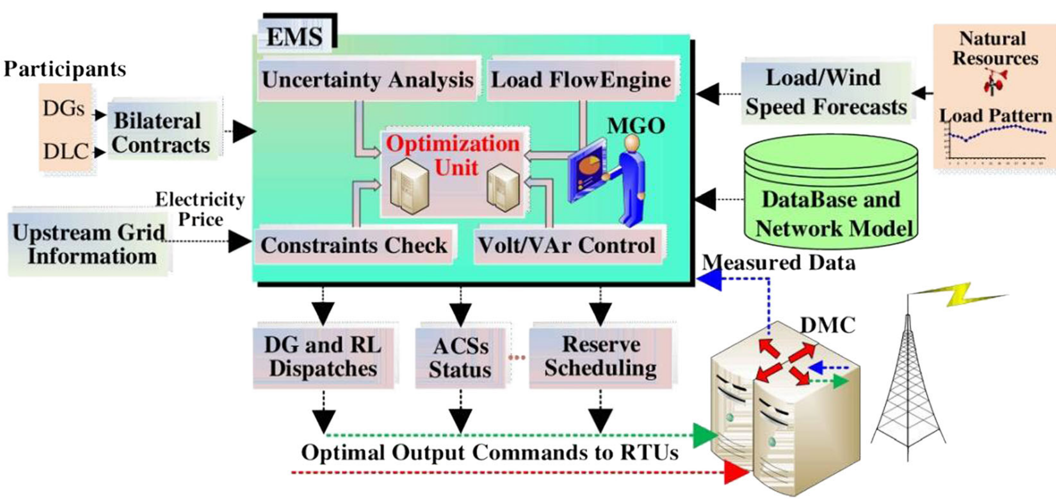

Figure 2. Structure of the proposed EMS.

DOI: 10.1002/er

MGO establishes efficient algorithms for predicting the next 24-h electricity prices in upstream grid. Furthermore, the MGO may also sign bilateral contracts with RLs or DGs to cooperate in incentive-based programs, such as load reduction or generation curtailment. These tools are efficient mechanisms in order to effectively reduce the emergency peak load conditions, mitigate power mismatches, and manage unforeseen feeder outages. The central core of the EMS is an optimization unit using a combination of software applications. A load flow engine executes a power flow on the whole network by which the Volt/VAr control practice and its technical constraints are suitably assessed. The EMS also establishes proper uncertainty evaluations to consider the forecasting errors both in load demand and natural resources. Then, the EMS yields the optimal output commands including upstream grid purchases, DGs and RLs dispatches, ACSs open or closed status, and reserve scheduling patterns.

3. PROPOSED FRAMEWORK FOR JOINT STOCHASTIC SCHEDULING OF ENERGY AND RESERVE

In short-term operational scheduling processes, the MGO is faced with different time-horizons [24]. As mentioned earlier, 24-h daily time frame is one of the most important horizons in which the MGO should determine its optimal interactions. To do so, the MGO reveals its forecasted load and renewable generations. Simultaneously, it determines the DG commitment patterns, RL participations, and suitable feeding network topologies. To accommodate the uncertainties, a joint energy and reserve scheduling paradigm is substantially required. The scheduled optimal reserve quantities make the MGO able to balance the power mismatches in real-time manners with low economical risk values. This notion improves the reliability of load serving by minimizing the EDNS index. In line with the smart grid innovations, a few recent studies are making up novel designs of energy exchanging mechanisms such as distributed energy trading. In these studies, the adjacent MGs are able to afford energy and ancillary services to their neighborhood MGs [25,26]. Thus, the determined energy and reserve values could be supplied through the upstream grid and voluntarily cooperation of adjacent MGs. Taking the aforementioned discussions into account, appropriate models are devised for accommodating load and wind speed forecasting errors based on a scenario-based approach. Then, for the basic deterministic case and also the stochastic scenarios, an EMS is wisely included based on the optimal load flow studies. To this end, a suitable objective function and the running constraints are formulated to achieve the optimal energy and reserve dispatching patterns.

3.1. Scenario generation approach

To integrate the probabilistic or so-called intermittent nature of wind speed behavior and load variations, different algorithms have been recommended in the literature. Monte Carlo analysis is known as the most accurate uncertainty modeling approach. However, handling a large number of scenarios makes it a highly time-consuming one. As the inclusion of topological reconfigurations in the scheduling process of MG makes it a sophisticated and combinatorial optimization problem, accurate enough models are deemed for uncertainty handling. In [27], Wang and Gooi have successfully applied a scenario-based probabilistic methodology for spinning reserve estimation considering renewable-based DGs. They have represented the uncertain nature of load and wind speed in the form of probability density functions (PDFs). Subsequently, by appropriate segmenting of the PDFs, sufficient scenarios are generated to be considered in scheduling process. Based on an acceptable performance, herein, a same approach is taken for uncertainty handling. The most common PDF used for representing the wind speed behavior is the Rayleigh PDF which is a simplified case of Weibull distribution [28]. For the purpose of observing the uncertain nature of wind speed, the Rayleigh PDF at each hour is divided into several discrete intervals, whose number is determined by the desired accuracy. As Figure 3 (a) demonstrates, a five-interval PDF is utilized to suitably represent the forecasted hourly wind speed. Regarding the hourly forecasted load variations, there would be some deviations because of the partial imperfectness of the forecasting mechanism. These uncertainties are regularly modeled using normal PDF [29]. A similar approach to the case of wind speed is taken into account. Herein, a seven-interval discretized PDF represents the forecasted values of load demand at each hour. This process is depicted in Figure 3 (b). The probability of occurrence for each interval, which is defined based on the concept of states, is calculated as the area between those specific margins. For the ease of analysis, the average value of each discrete interval is appointed as the indicator of that interval. The scenario tree model with lower computational burden and enough degree is implemented to generate the scenarios. By representing the load and wind speed uncertainties respectively with five and seven probable states, 35 scenarios are generated at each hour.

3.2. Mathematical modeling of the proposed EMS

3.2.1. Objective function

Versatile objectives could be implemented by the EMS in daily operational manner; however, the most important one is the minimization of MG's total operation costs.

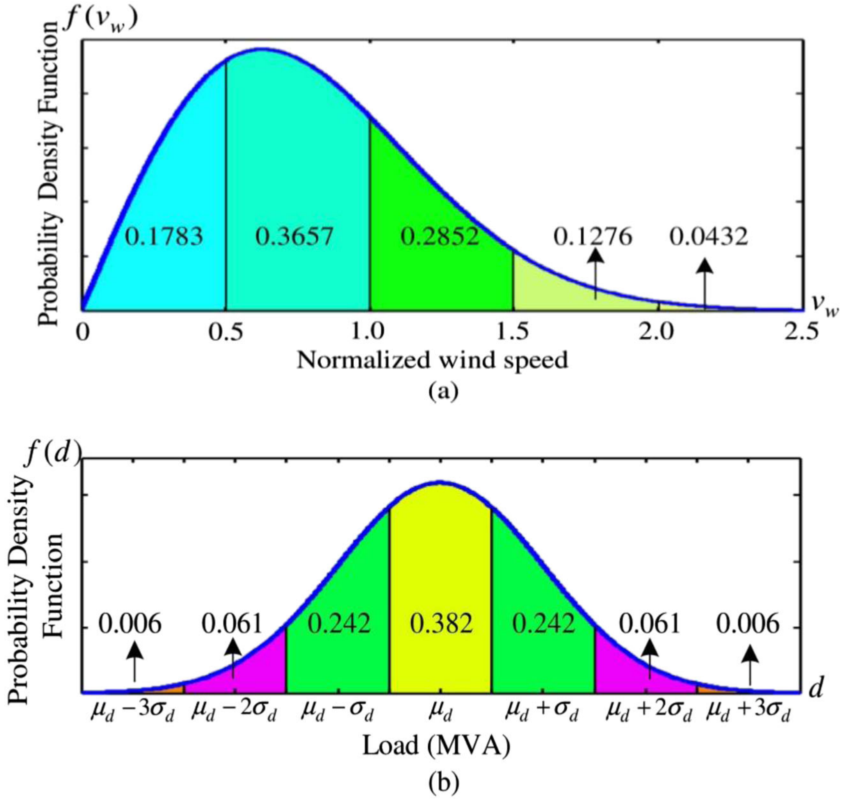

Figure 3. (a): Rayleigh PDF for wind speed; (b): Normal PDF for load variations.

The optimization problem is, therefore, formulated as follows:

$$
\begin{aligned}
\text{Minimize } \mathrm{F}(\mathbf{x},\ \mathbf{u}) = \sum_{t\in T}\Bigg(&\overbrace{\sum_{s\in S}\rho_t^{\mathrm{UG}}P_{t,s}^{\mathrm{UG}}}^{(\mathrm{a})} + \overbrace{\sum_{g\in G}C_{t,g,p}^{\mathrm{DG}}}^{(\mathrm{b})} \\
&+ \overbrace{\sum_{l\in L}\rho_t^{\mathrm{RL}}P_{t,l}^{\mathrm{RL}}}^{(\mathrm{c})} + \overbrace{\sum_{s\in S}k_q^{\mathrm{UG}}\rho_t^{\mathrm{UG}}Q_{t,s}^{\mathrm{UG}}}^{(\mathrm{d})} + \overbrace{\sum_{g\in G}C_{t,g,q}^{\mathrm{DG}}}^{(\mathrm{e})} \\
&+ \overbrace{\sum_{l\in L}k_q^{\mathrm{RL}}\rho_t^{\mathrm{RL}}Q_{t,l}^{\mathrm{RL}}}^{(\mathrm{f})} + \overbrace{\sum_{s\in S}\rho_{t,res}^{\mathrm{UG}}P_{t,s,res}^{\mathrm{UG}}}^{(\mathrm{g})} + \overbrace{\sum_{g\in G}C_{t,g,p,res}^{\mathrm{DG}}}^{(\mathrm{h})} \\
&+ \overbrace{\sum_{l\in L}\rho_{t,res}^{\mathrm{RL}}P_{t,l,res}^{\mathrm{RL}}}^{(\mathrm{i})} + \overbrace{\sum_{s\in S}k_q^{\mathrm{UG}}\rho_{t,res}^{\mathrm{UG}}Q_{t,s,res}^{\mathrm{UG}}}^{(\mathrm{j})} + \overbrace{\sum_{g\in G}C_{t,g,q,res}^{\mathrm{DG}}}^{(\mathrm{k})} \\
&+ \overbrace{\sum_{l\in L}k_q^{\mathrm{RL}}\rho_{t,res}^{\mathrm{RL}}Q_{t,l,res}^{\mathrm{RL}}}^{(\mathrm{l})} + \overbrace{\sum_{g\in G}X_{t,g}\mathrm{SU}_g}^{(\mathrm{m})} + \overbrace{\sum_{g\in G}Z_{t,g}\mathrm{SD}_g}^{(\mathrm{n})} \\
&+ \overbrace{VOLL\times EDNS_t}^{(\mathrm{o})}\Bigg) + \overbrace{\sum_{k\in K}C^{\mathrm{SW}}N_{ACS_k}^{\mathrm{SW}}}^{(\mathrm{p})}.
\end{aligned} \tag{1}
$$

In (1), vectors **x** and **u** are denoting the control and dependent variables as follows.

$$
\begin{aligned}
\mathbf{x} = \big[&P_s^{\mathrm{UG}}, Q_s^{\mathrm{UG}}, P_{s,res}^{\mathrm{UG}}, Q_{s,res}^{\mathrm{UG}}, P_g^{\mathrm{DG}}, Q_g^{\mathrm{DG}}, P_{g,res}^{\mathrm{DG}}, Q_{g,res}^{\mathrm{DG}} \\
&P_l^{\mathrm{RL}}, Q_l^{\mathrm{RL}}, P_{l,res}^{\mathrm{RL}}, Q_{l,res}^{\mathrm{RL}}, \overline{\mathbf{ACS}}\big]
\end{aligned} \tag{2}
$$

$$\overline{\mathrm{ACS}} = [ACS_1, ACS_2, \ldots, ACS_{N_{br}}] \tag{3}$$

$$\mathbf{u} = \left[\overline{|\mathbf{V}|}, \overline{|\mathbf{S}_f|}\right] \tag{4}$$

Different cost terms are included in the objective function (1). The costs of purchasing active power from external grid, DGs dispatches, and contracting with RLs to reduce their consumption are represented by the terms designated with (a), (b), and (c). Term (b) as the production cost of DGs is represented as:

$$C_{t,g,p}^{\mathrm{DG}} = W_{t,g}a_g + b_gP_{t,g}^{\mathrm{DG}} + c_g\left(P_{t,g}^{\mathrm{DG}}\right)^2. \tag{5}$$

Continued in (1), (d), (e), and (f) are respectively accounted for the costs of reactive power provision by external grid, DGs, and RLs, respectively. Grid code connection requirements necessitates DGs to have mandatory cooperation in reactive power support without financial compensation. By this strategy, they should be operated in power factors (PFs) extending from 0.95 lagging to 0.95 leading [30]. On the other hand, if the network status requires higher support of reactive power by DGs, their PFs would drop down from the designated ranges. Hence, monetary reimbursements represented in (6) are necessary because of lost opportunity cost [31].

$$C_{t,g,q} = k_q^{\mathrm{DG}} I_{t,g} \left[C_{t,g,p}\left(S_{g,max}^{\mathrm{DG}}\right) - C_{t,g,p}\left(\sqrt{\left(S_{g,max}^{\mathrm{DG}}\right)^2 - \left(Q_{t,g}^{\mathrm{DG}}\right)^2}\right)\right] \tag{6}$$

Returning to (1), terms (g), (h), and (i) are denoting the costs originating because of active power reserve provisions for covering the uncertainties. In a similar approach, terms (j), (k), and (l) are representing the costs of reactive power reserve provisions. Terms (m) and (n) are respectively representing the start up and shut down costs of DGs. Considering possible scenarios, it is possible to encounter demand not-supplied status because of the imbalance of generation and consumption patterns. In this regard, term (o) is the economical statement of the EDNS index considering the value of lost load (VOLL). Ultimately, the last term identified by (p) is the daily switching costs because of topological reconfigurations through ACSs.

3.2.2. Constraints

The active and reactive power load flow equations are appropriately modified to include the presence of DGs and RLs in active and reactive power generations. As well, the demand-not-supplied parameters are included in analyzing the load flow equations in different scenarios.

$$\begin{aligned} &P_{t,s,\omega}^{\mathrm{UG}} + \sum_{g\in G_i} P_{t,g,\omega}^{\mathrm{DG}} + \sum_{w\in W_i \& \omega\in\Omega} P_{t,w,\omega}^{\mathrm{WT}} + P_{t,i,\omega}^{\mathrm{RL}} \\ &+DNS_{p,t,\omega} - P_{t,i,\omega}^{\mathrm{D}} - \sum_{f\in F \& j\in B} P_{t,ij}^{f}\left(V_i,, V_j,, Y_{ij},, \theta_{ij}\right) = 0 \end{aligned} \tag{7}$$

$$\begin{aligned} &Q_{t,s,\omega}^{\mathrm{UG}} + \sum_{g\in G_i} Q_{t,g,\omega}^{\mathrm{DG}} + Q_{t,i,\omega}^{\mathrm{RL}} \\ &+DNS_{q,t,\omega} - Q_{t,i,\omega}^{\mathrm{D}} - \sum_{f\in F \& j\in B} Q_{t,ij}^{f}\left(V_i,, V_j,, Y_{ij},, \theta_{ij}\right) = 0 \end{aligned} \tag{8}$$

Considering the required reserve provisions, the active and reactive powers provided by substations, DGs, and RLs in a specific scenario are respectively regarded as follows:

$$P_{t,s,\omega}^{\mathrm{UG}} = P_{t,s}^{\mathrm{UG}} + P_{t,s,res}^{\mathrm{UG}} \tag{9}$$

$$Q_{t,s,\omega}^{\mathrm{UG}} = Q_{t,s}^{\mathrm{UG}} + Q_{t,s,res}^{\mathrm{UG}} \tag{10}$$

$$\sum_{g\in G_i} P_{t,g,\omega}^{\mathrm{DG}} = \sum_{g\in G_i} P_{t,g}^{\mathrm{DG}} + \sum_{g\in G_i} P_{t,g,res}^{\mathrm{DG}} \tag{11}$$

$$\sum_{g\in G_i} Q_{t,g,\omega}^{\mathrm{DG}} = \sum_{g\in G_i} Q_{t,g}^{\mathrm{DG}} + \sum_{g\in G_i} Q_{t,g,res}^{\mathrm{DG}} \tag{12}$$

$$P_{t,i,\omega}^{\mathrm{RL}} = P_{t,i}^{\mathrm{RL}} + P_{t,i,res}^{\mathrm{RL}} \tag{13}$$

$$Q_{t,i,\omega}^{\mathrm{RL}} = Q_{t,i}^{\mathrm{RL}} + Q_{t,i,res}^{\mathrm{RL}}. \tag{14}$$

3.2.2.1. *Upstream grid purchase constraint.*

The transformer's capacity would impose a constraint on the maximum amount of both energy and reserve power imported from external grid.

$$\left[\left(P_{t,s}^{\mathrm{UG}} + P_{t,s,res}^{\mathrm{UG}}\right)^2 + \left(Q_{t,s}^{\mathrm{UG}} + Q_{t,s,res}^{\mathrm{UG}}\right)^2\right]^{1/2} \le S_{s,\max}^{\mathrm{UG}} \quad \forall s\in S \tag{15}$$

3.2.2.2. *DG generation limits.*

These caps are included to schedule DGs bounding their dispatched power within their rated capacities. Also, DGs should meet permissible range for PFs.

$$P_{g,\min}^{\mathrm{DG}} \le P_{t,g}^{\mathrm{DG}} + P_{t,g,res}^{\mathrm{DG}} \le P_{g,\max}^{\mathrm{DG}} \quad \forall g\in G \tag{16}$$

$$Q_{g,\min}^{\mathrm{DG}} \le Q_{t,g}^{\mathrm{DG}} + Q_{t,g,res}^{\mathrm{DG}} \le Q_{g,\max}^{\mathrm{DG}} \quad \forall g\in G \tag{17}$$

$$\left[\left(P_{t,g}^{\mathrm{DG}} + P_{t,g,res}^{\mathrm{DG}}\right)^2 + \left(Q_{t,g}^{\mathrm{DG}} + Q_{t,g,res}^{\mathrm{DG}}\right)^2\right]^{1/2} \le S_{g,\max}^{\mathrm{DG}} \quad \forall g\in G \tag{18}$$

$$PF_{t,g}^{\mathrm{DG}} = \frac{\left(P_{t,g}^{\mathrm{DG}} + P_{t,g,res}^{\mathrm{DG}}\right)}{\left[\left(P_{t,g}^{\mathrm{DG}} + P_{t,g,res}^{\mathrm{DG}}\right)^2 + \left(Q_{t,g}^{\mathrm{DG}} + Q_{t,g,res}^{\mathrm{DG}}\right)^2\right]^{1/2}} \quad \forall g\in G \tag{19}$$

$$PF_{g,\min}^{\mathrm{DG}} \le PF_{t,g}^{\mathrm{DG}} \le PF_{g,\max}^{\mathrm{DG}} \quad \forall g\in G \tag{20}$$

3.2.2.3. *RL constraints.*

RLs are supposed to be operated with constant PFs. Also, the contribution of RLs in both energy and reserve provisions is limited as the contacted amounts.

$$0 \le P_{t,i}^{\mathrm{RL}} + P_{t,i,res}^{\mathrm{RL}} \le P_{t,l,\max}^{\mathrm{RL}} \quad \forall l\in L \tag{21}$$

$$Q_{t,i}^{\mathrm{RL}} = \tan\left(\cos^{-1}\left(PF_i^{\mathrm{RL}}\right)\right) \times P_{t,i}^{\mathrm{RL}} \quad \forall l\in L \tag{22}$$

$$Q_{t,i,res}^{\mathrm{RL}} = \tan\left(\cos^{-1}\left(PF_i^{\mathrm{RL}}\right)\right) \times P_{t,i,res}^{\mathrm{RL}} \quad \forall l\in L \tag{23}$$

3.2.2.4. *Flow limits on feeders.*

The power carrying capacity should be capped through each feeder to preserve the thermal rating constraints. That is,

$$\left[\left(P_{t,ij}^{f}\right)^2 + \left(Q_{t,ij}^{f}\right)^2\right]^{\frac{1}{2}} \le S_{\max}^{f} \quad \forall f\in F. \tag{24}$$

3.2.2.5. *Bus voltage limits.*

The following constraint confirms an acceptable voltage profile for all buses.

$$V_{\min} \leq \left|V_{t,i}\right| \leq V_{\max} \qquad \forall i \in B \tag{25}$$

3.2.2.6. Network radiality and switching limitations of ACSs. To feature a radial structure for the network, the total number of main loops should be kept constant, represented in (26). The depth first search algorithm is implemented to assure radial structures for the network [32]. Also, equations 27, 28 are considered to limit the switching actions of each ACS in its daily switching actions.

$$N_{mL} = N_{br} - N_{bus} + 1 \qquad \forall t \in T \tag{26}$$

$$N_{ACS_k}^{\mathrm{SW}} = \sum_{t} \mathrm{abs}\left(ACS_{k,t} - ACS_{k,t-1}\right) \tag{27}$$

$$N_{ACS_k}^{\mathrm{SW}} \leq N_{\max}^{\mathrm{SW}} \tag{28}$$

3.2.3. EDNS calculation approach

For a possible solution vector **x**, a probable decrease in wind speed and its power generation as well as an unforeseen increase in load demand of MG might result in inequality of demand and supply. At a specific hour, EDNS is calculated on all scenarios taking into account the power and demand equality constraints namely (7) and (8). Based on the established approach, the energy and reserve scheduling is implemented simultaneously. The proposed solutions for reserve provisions are supplemented to the obtained values for energy products as in (9)–(14). Then, an internal process based on optimal power flow is devoted to assess the performance of the proposed solution on each scenario and calculate the EDNS value. Having determined the demand not supplied (DNS) values in all scenarios and considering their probability of occurrence, EDNS is calculated based on (29) and (30).

$$\pi_{t,\omega} = \pi_{t,w_s} \times \pi_{t,d_s} \tag{29}$$

$$EDNS_t = \sum_{\omega} \pi_{t,\omega} \times DNS_{t,\omega} \qquad \forall \omega \in \Omega \tag{30}$$

3.2.4. Optimization technique

Considering the continuous and discrete variables, the founded framework for joint stochastic energy and reserve scheduling represents a mixed-integer non-linear problem. Some related surveys have benefitted from commercial solvers such as DICOPT in GAMS to solve such problems [19,33]. However, these classical solvers usually fail to find the optimum solutions especially in mixed-integer non-linear problems [34]. Hence, the intelligent optimization methods have been regarded as suitable alternatives more recently [35,36]. Based on the well performance of these algorithms, this study has deployed the genetic algorithm (GA) for solving the proposed optimization procedure. GA is an intelligent search technique which imitates the biological selection process in nature. In this course, the most qualified parents have the greatest chance to stay alive and duplicate themselves. By stochastic iterative generations and then evaluating their characteristics, GA probes the search space meticulously to determine the optimal solutions [37].

4. NUMERICAL ANALYSIS

This section presents several numerical studies to scrutinize the performance of the proposed EMS in daily energy and reserve commitments.

4.1. Test system

In order to conduct the numerical analysis on the proposed approach, a well-organized MG is required. Reference [38] has conducted a study on a MG hosting DGs and WTs. This is worth noting that the referred system is launched as the test case in similar studies such as [39,40]. Based on the aforementioned explanations, the same MG is elected as the test system herein. Figure 4 demonstrates the single line diagram of this system for which the basic data are available in [41]. The connection buses of four DGs are determined as nodes 8, 13, 16, and 25 whose ratings and technical features are reported in Table I. Also, to improve the overall efficiency of DGs, they are dispatched over than 25% of their ratings [42]. Otherwise, they are not switched on. Moreover, the specified range for leading or lagging minimum PF is considered as 0.85.

Four units of WTs with rated power of 3 MW are supplemented in the network at nodes 14, 16, 31, and 33. The daily wind speed forecasts are represented in Figure 5. Five largest loads are contracted as RLs located at nodes 8, 14, 24, 30, and 32 that could be decreased up to 10% during the day. Figure 6 exhibits the price for 1 MW decrease by RLs. Also, the VOLL is set at 1200 $/MVA for the case of demand not supplied happening.

The MG encompasses five maneuver tie-lines. Each feeder branch is equipped with ACSs to attain flexible topologies in stochastic scheduling process of the network. Bus 1, as the main substation, represents the connecting point of MG to the upstream grid. Different RTUs are mounted in MG to provide efficient online communication capabilities. Taking a lifetime of 15 years for ACSs [43], the possible daily switching operations of each ACS is determined as six among which four switchings are allocated to the reconfiguration practice and two operations are assigned for protection and isolation duty, maintenance outages, or other tasks. The investment and maintenance costs of ACSs brings 1$ cost per each switching action [44]. Sample daily electricity prices on July 16, 2013 on NYISO are used as the external grid prices to study the proposed stochastic scheduling framework [45]. Figure 7 illustrates the daily

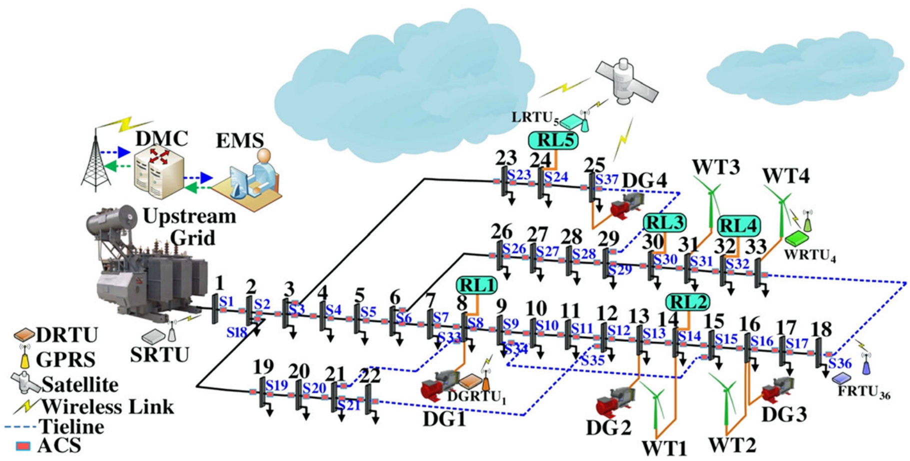

Figure 4. Single line diagram of the test case MG.

Table I. Cost coefficients and technical data for DG units.

DG unit	Cost function coefficients					Technical constraints	
	a_g (\$)	b_g (\$/MW)	c_g (\$/MW^2)	SU_g (\$)	SD_g (\$)	$P_{g,min}$ (MW)	$S_{g,max}$ (MVA)
DG1	27	79	0.0035	15	10	1	4.12
DG2	25	87	0.0045	15	10	1	3.53
DG3	28	92	0.0045	15	10	1	3.53
DG4	26	81	0.0035	15	10	1	4.83

electricity prices while the network total load is demonstrated in Figure 8.

4.2. Discussions on numerical results

Different scheduling strategies are devised to interrogate the performance of the proposed stochastic operational framework. Having provided a brief preface of each strategy, complete comparative discussions are made.

4.2.1. Energy and reserve scheduling considering a fixed topology of MG

This strategy is referred as the *base case* where MGO endeavors to optimally schedule the energy and reserve commitments in MG without the possibility of remotely network reconfigurations, i.e. the network is not equipped with ACSs.

4.2.2. Energy and reserve scheduling considering MG's reconfigurations through ACSs

In the second strategy which is expressed as *with reconfiguration*, the MGO includes the presence of ACSs in optimal energy and reserve scheduling of active elements. As well, it simultaneously assigns the optimal switching sequences for the network topology.

The performance of the proposed operational scheduling framework in optimal grid purchases, dispatching of DGs, and RLs commitment is demonstrated in Figures 9–11. As it is seen, the daily time horizon is mainly divided into two operating periods. Off-peak period includes the hours between 1 to 12 and 20 to 24, and the peak load interval corresponds to the hours between 13 and 19. With respect to Figures 9 and 10, it can be observed that at the off-peak periods and in the base case strategy, both the external grid and DGs are the main scheduled resources for supplying the requirements of MG. It is while; the participation of RLs is to some extent low because of the higher contract prices, as depicted in Figure 11. In the base case, the higher commitment of RLs at off-peak hours including 20 to 24 originates because of the heavy load of the MG as well as the decrease in wind speed. At the peak hours and sweeping from 13 to 19 in the base case, it is evident that all of the

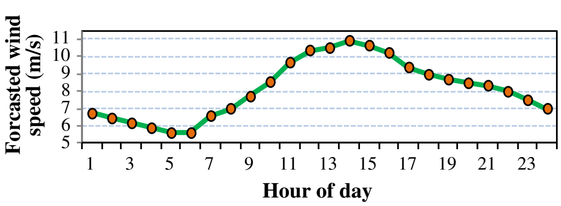

Figure 5. Daily wind speed forecasts.

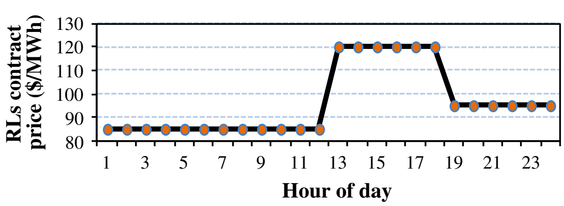

Figure 6. Contracted price of 1 MW decrease by RLs during the day.

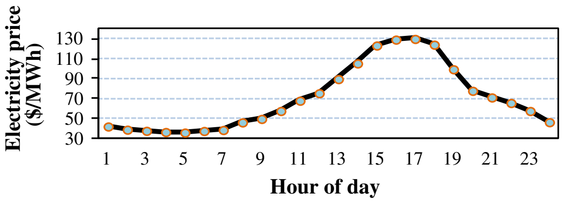

Figure 7. Daily electricity prices in upstream grid.

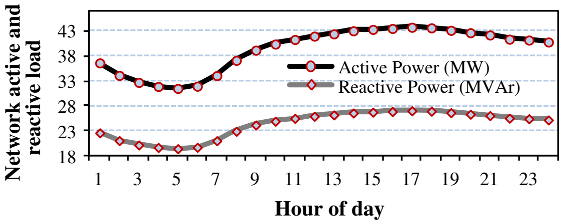

Figure 8. Forecasted daily load profile of the MG.

active elements have a remarkable share in supplying MG's demand. However, because of higher prices by the external grid, DGs are dispatched nearly at their maximum capacities. Thereby, the external grid and RLs are respectively the most triggered resources. Interrogating the second strategy, Figures 9–11 reveal that by applying network reconfiguration through ACSs and obtaining more suitable paths for power flows, there is a great change in dispatching patterns of elements. At off-peak hours, as the price of electricity production by DGs is higher than the power transfer from the external grid, the topology optimization of the MG impressively elevates the share of external grid in power provision. In spite, this trend declines the participation of both DGs and RLs at these hours. At the peak hours, the reconfiguration process allows the highest dispatched power from DGs, while the provided power from the external grid and RLs experiences a soft decrease. The foregoing results are also evidence for changes in unallocated capacities as the reserve resources in accommodating the probable uncertainties.

In the base case, noting that the reserve prices of DGs and RLs at peak hours are lower than the external grid's, Figure 12 illustrates that the unallocated capacities of these resources are committed as the required reserve power. In contradiction, the external grid is the main resource of reserve provision at off-peak hours. A fine attention on the obtained results in Figures 9–11 reveals that at off-peak hours, the MG's reconfiguration process decreases the unallocated capacity of substation. On the other hand, the reconfiguration strategy results in increased unallocated capacities of DGs and RLs at off-peak hours. Thus, Figure 13 illustrates that at off-peak hours including 10 to 12 and 21

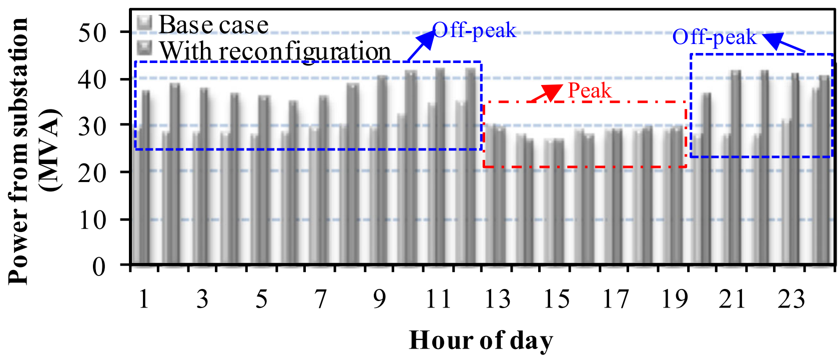

Figure 9. Optimal grid purchases.

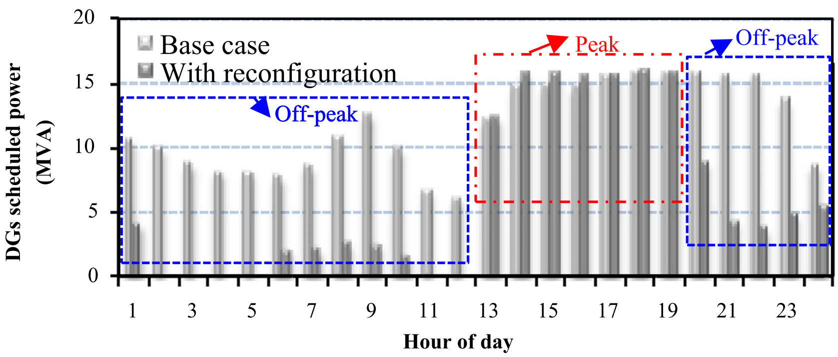

Figure 10. Optimal schedule of DGs.

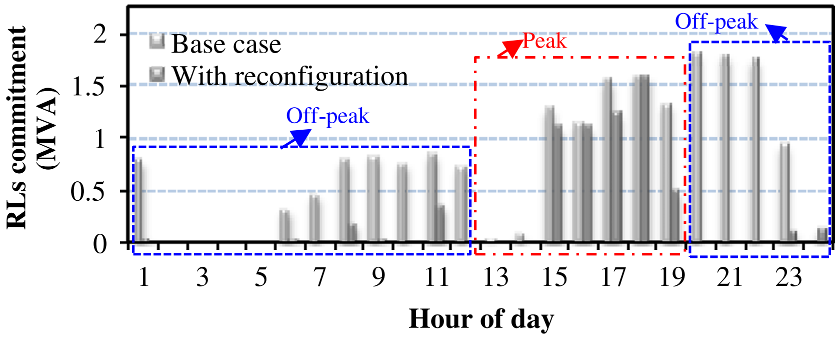

Figure 11. Optimal commitment of RLs.

to 24, the required reserve power is mainly furnished by DGs as they are the cheaper resources. It is worthy to note that as the costs of RLs at the peak hours are lower than the external grid's, the unallocated capacities of RLs are scheduled as the reserve power.

Regarding the economical issues and thanks to the topological changes through ACSs, a significant cost drop is seen at off-peak hours because of DGs lower dispatching. Results are shown in Figure 14. For the peak hours, there is not any remarkable cost reduction following the MG's reconfigurations. At these hours, both of the DGs and RLs are dispatched approximately at their maximum ratings. The total operation cost for the base case and the case with reconfiguration are equal to 65 228 $ and 60 455 $, respectively. It can be seen that by deploying ACSs in optimal stochastic operational scheduling of MG, there will be a 7.3% decrease in total operation costs. Such an achievement is a meaningful metric in enhancing the operational scheduling of MGs.

Table II demonstrates the optimally tuned switching actions for each ACS. It can be deduced that the obtained topologies are the same for some hours during the day. Such an observation is because of limiting the maximum switching actions throughout a day. Hence, the switching limitations are effectively fulfilled by the established EMS as well.

4.3. Result validation

It is necessary to mention that the proposed approach is implemented utilizing a PC with 2.53-GHz CPU and 4-GB of RAM. As the founded framework is a non-linear

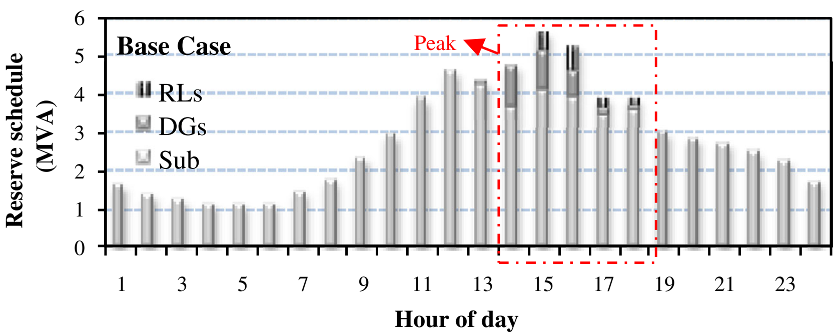

Figure 12. Reserve scheduling in the base case.

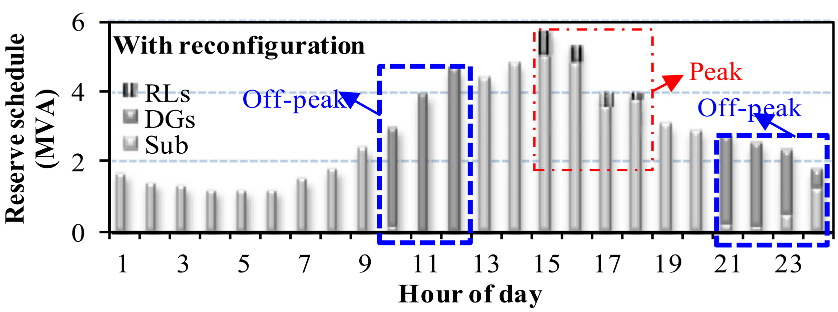

Figure 13. Reserve scheduling considering MG's structural reconfigurations.

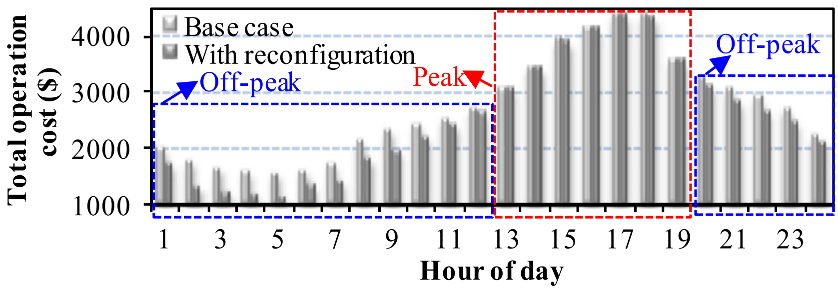

Figure 14. Daily operational costs of MG.

one combined with binary variables, the GA approach is concerned with optimality issues. For getting far from the local optima and approaching toward the global optima, the investigated system is assessed in several distinct executions with population size of 50 and 1000 iterations. Although demonstrating negligible differences in different runs, however, the best results are attained with a mutation rate of 0.01 and crossover rate of 0.5. The solution time could be obtained as lower than 300 s which is an acceptable time for daily scheduling of a MG.

5. CONCLUDING REMARKS AND THE FUTURE WORKS

This study intended to address an optimal joint stochastic energy and reserve scheduling framework for MGs. An innovative step toward the fulfillment of EMS capabilities has been the inclusion of flexible network topologies in scheduling of MGs. Likewise, the uncertainties regarding the forecasting errors of load and wind speed have been adopted in the proposed framework. Based on the numerical analysis, it can be deduced that including ACSs in scheduling of MGs would pose substantial effects in optimal daily energy and reserve dispatching patterns. By reconfiguring the network, EMS lowers the participation of DGs and RLs during the off-peak hours with lower electricity prices of the external grid. Meanwhile, by determination of the optimal switching sequences for ACSs and then altering the network topology, EMS settles more suitable patches for higher electricity transfer from the external grid. This trend results in released capacity of DGs and RLs which could be taken in use for reserve provision. Such performance was seen during the hours between 10–12 and 21–24. Also, RLs have been committed as reserve resources at peak hours when the contracted prices are lower than the external grid. Specifically speaking, implementing the hourly flexible topologies of MG results in significant improvements in its economical metrics. In this regard, a record of 7.3% reduction in the MG's total daily operation costs is achieved. The obtained results approve the merits of integrating MG's topological variations in optimal energy and reserve commitments.

Table II. Open ACSs in reconfiguration process.

Hours	Open ACSs in reconfiguration process
1	7-10-12-28-29
2–5	7-9-14-31-37
6–9	6-10-14-29-37
10–13	7-10-13-31-37
14–19	6-10-12-28-30
20–22	7-9-14-28-32
23–24	7-10-12-28-29

The investigated framework is still a challenging one in dealing with some novel concepts such as energy mobility issues by electric vehicles. These notions are open topics as the future steps in efficient EMS designs.

NOMENCLATURE

t,T	=	Index and set of time intervals.
i, j, B, N_{bus}	=	Indices, set, and total number of buses.
f, F, N_{br}	=	Index, set, and total number of feeders.
w, W	=	Index and set of wind turbines.
ω, Ω	=	Index and set of scenarios.
s, S	=	Index and set of substations.
l, L	=	Index and set of responsive loads (RLs).
k, K	=	Index and set of automatically controlled switches (ACSs).
g, G, G_i	=	Index and set of distributed generations (DGs), and set of DGs at bus i.
ρ^{UG}	=	Electricity price of upstream grid.
ρ^{RL}	=	Contract price of RL's participation.
ρ^{UG}_{res}	=	Reserve price of upstream grid.
ρ^{RL}_{res}	=	Contracted reserve price by RLs.
C^{DG}_p	=	Cost function for DG's active power production.
C^{DG}_q	=	Cost function for DG's reactive power production.
a, b, c	=	Cost function coefficients of DGs.
SU, SD	=	Start-up and shut-down costs of DGs.
k^{UG}_q	=	Coefficient for reactive power price by upstream grid.

k_q^{DG} = Coefficient for DG's reactive power cost.
k_q^{RL} = Coefficient for RL's reactive power price.
$P^{\mathrm{D}}, Q^{\mathrm{D}}$ = Active and reactive power demand at each bus.
Y, θ = Magnitude and phase angle of feeder's admittance.
$S_{\max}^{\mathrm{UG}}$ = Substation's maximum apparent power capacity.
$P_{\max}^{\mathrm{DG}}, P_{\min}^{\mathrm{DG}}$ = DG's maximum and minimum active power limits.
$Q_{\max}^{\mathrm{DG}}, Q_{\min}^{\mathrm{DG}}$ = DG's maximum and minimum reactive power limits.
$S_{\max}^{\mathrm{DG}}$ = DG's maximum apparent power capacity.
$PF_{\max}^{\mathrm{DG}}, PF_{\min}^{\mathrm{DG}}$ = DG's maximum and minimum power factors.
$P_{\max}^{\mathrm{RL}}$ = Maximum power reduction by RL.
PF^{RL} = Constant power factor for RL.
$S_{\max}^{f}$ = Feeder's maximum apparent power flow capacity.
$V_{\max}, V_{\min}$ = Maximum and minimum limits of bus voltage.
R_{ij}, X_{ij} = Resistance and reactance of feeder between buses i and j.
N_{mL} = Number of main loops in the network.
$N_{\max}^{\mathrm{SW}}$ = Maximum number of daily switching actions for each ACS.

π_{ws} = Probability of occurrence for each wind state.
π_{ds} = Probability of occurrence for each load state.
π = Probability of occurrence for each scenario.
P^{WT} = Active power generation by a WT unit.
$P^{\mathrm{UG}}, Q^{\mathrm{UG}}$ = Active and reactive power purchases from upstream grid.
$P^{\mathrm{DG}}, Q^{\mathrm{DG}}$ = DG's active and reactive power dispatches.
$P^{\mathrm{RL}}, Q^{\mathrm{RL}}$ = RL's active and reactive power participations.
$P_{res}^{\mathrm{UG}}, Q_{res}^{\mathrm{UG}}$ = Active and reactive power reserve provisions through upstream grid.
$P_{res}^{\mathrm{DG}}, Q_{res}^{\mathrm{DG}}$ = DG's active and reactive power reserve provisions.
$P_{res}^{\mathrm{RL}}, Q_{res}^{\mathrm{RL}}$ = RL's active and reactive power reserve provisions.
PF^{DG} DG's = Adaptive power factor.
V_i = Voltage phasor at i-th bus.
S^f = Apparent power flow through f-th feeder.
P^f, Q^f = Active and reactive power flows through f-th feeder.
ACS = Automatically controlled switch status.
N_{ACS}^{SW} = Number of daily switching actions for each ACS.
W, X, Z = Binary variables for DG's commitment, start-up, and shut-down status.
I = Binary variable denoting that the power factor of a DG unit is beyond the mandatory region.

REFERENCES

1. Garcia P, Garcia CA, Fernandez LM, Llorens F, Jurado F. ANFIS-based control of a grid-connected hybrid system integrating renewable energies, hydrogen and batteries. *IEEE Trans. Ind. Inform.* 2014; **10**:1107–1117.
2. Wang F, Hedman KW. Dynamic reserve zones for day-ahead unit commitment with renewable resources. *IEEE Transactions on Power Systems* 2015; **30**:612–620.
3. Palensky P, Dietrich D. Demand side management: demand response, intelligent energy systems, and smart loads. *IEEE Trans. Ind. Inform.* 2011; **7**:381–388.
4. Gungor VC, Sahin D, Kocak T, Ergut S, Buccella C, Cecati C, Hancke GP. A survey on smart grid potential applications and communication requirements. *IEEE Trans. Ind. Inform.* 2013; **9**:28–42.
5. Hamilton B, Summy M. Benefits of the smart grid [in my view]. *IEEE Power Energy Mag.* 2011; **9**:102–104.
6. Shahidehpour M, Yamin H, Li Z. *Market overview in electric* power *systems*. *Wiley-IEEE Press* 2002; **1–20**.
7. M.H. Tackett, Experience with implementing simultaneous co-optimization in the Midwest ISO energy and operating reserve markets *IEEE/PES Power Systems Conference and Exposition*, *PSCE'09*. 2009; 1–2.
8. Graditi G, Di Silvestre ML, Gallea R, Riva Sanseverino E. Heuristic-based shiftable loads optimal management in smart micro-grids. *IEEE Trans. Ind. Inform.* 2015; **11**:271–280.
9. Strasser T, Siano P, Vyatkin V. Guest editorial. New trends in intelligent energy systems-an industrial informatics points of view. *IEEE Trans. Ind. Inform.* 2015; **11**:207–209.
10. Vrba P, Marik V, Siano P, Leitao P, Zhabelova G, Vyatkin V, Strasser T. A review of agent and service-oriented concepts applied to intelligent energy systems. *IEEE Trans. Ind. Inform.* 2014; **10**:1890–1903.
11. Widl E, Palensky P, Siano P, Rehtanz C. Guest editorial. Modeling, simulation, and application of cyber-

physical energy systems. *IEEE Trans. Ind. Inform.* 2014; **10**:2244–2246.
12. Siano P. Evaluating the impact of registered power zones incentive on wind systems integration in active distribution networks. *IEEE Trans. Ind. Inform.* 2015; **11**:523–530.
13. Siano P, Cecati C, Yu H, Kolbusz J. Real time operation of smart grids via FCN networks and optimal power flow. *IEEE Trans. Ind. Inform.* 2012; **8**:944–952.
14. Cecati C, Citro C, Piccolo A, Siano P. Smart operation of wind turbines and diesel generators according to economic criteria. *IEEE Transactions on Industrial Electronics* 2011; **58**:4514–4525.
15. Ding YM, Hong SH, Li XH. A demand response energy management scheme for industrial facilities in smart grid. *IEEE Trans. Ind. Inform.* 2014; **10**:2257–2269.
16. Kilkki O, Alahaivala A, Seilonen I. Optimized control of price-based demand response with electric storage space heating. *IEEE Trans. Ind. Inform.* 2015; **11**:281–288.
17. Bottura R, Borghetti A. Simulation of the Volt/Var control in distribution feeders by means of a networked multiagent system. *IEEE Trans. Ind. Inform.* 2014; **10**:2340–2353.
18. Safdarian A, Fotuhi-Firuzabad M, Lehtonen M. A stochastic framework for short–term operation of a distribution company. *IEEE Transactions on Power Systems* 2013; **28**:4712–4721.
19. Zakariazadeh A, Jadid S, Siano P. Economic-environmental energy and reserve scheduling of smart distribution systems: a multi–objective mathematical programming approach. *Energy Conv. Mang.* 2014; **78**:151–164.
20. Mohan V, Govind Singh J, Ongsakul W. An efficient two stage stochastic optimal energy and reserve management in microgrid. *Applied Energy* 2015; **160**:28–38.
21. Mendes A, Boland N, Guiney P, Riveros C. Switch and tap-changer reconfiguration of distribution networks using evolutionary algorithms. *IEEE Transactions on Power Systems* 2013; **28**:85–92.
22. Siano P, Chen P, Chen Z, Piccolo A. Evaluating maximum wind energy exploitation in active distribution networks. *IET Gener. Transm. Dis.* 2010; **4**:598–608.
23. Rao RS, Ravindra K, Satish K, Narasimham SVL. Power loss minimization in distribution system using network reconfiguration in the presence of distributed generation. *IEEE Transactions on Power Systems* 2013; **28**:317–325.
24. Logenthiran T, Srinivasan D, Khambadkone AM, Aung HN. Multiagent system for real-time operation of a microgrid in real-time digital simulator. *IEEE Transactions on Smart Grid* 2012; **3**:925–933.
25. Wu Y, Tan X, Qian L, Tsang DHK, Song WZ, Yu L. Optimal pricing and energy scheduling for hybrid energy trading market in future smart grid. *IEEE Trans. Ind. Inform.* 2015; **1–11**.
26. Gregoratti D, Matamoros J. Distributed energy trading: the multiple-microgrid case. *IEEE Transactions on Industrial Electronics* 2015; **62**:2551–2559.
27. Wang MQ, Gooi HB. Spinning reserve estimation in microgrids. *IEEE Transactions on Power Systems* 2011; **26**:1164–1174.
28. Liang H, Tamang AK, Zhuang W, Shen XS. Stochastic information management in smart grid. *IEEE Commun. Surv. & Tut.* 2014; **16**:1746–1770.
29. Ding N, Besanger Y, Wurtz F. Next-day MV/LV substation load forecaster using time series method. *Electr. Pow. Syst. Res.* 2015; **119**:345–354.
30. FERC report, Reactive power resources Federal Energy Regulatory Commission, AD12-10-000, 2012. [Online]: http://www.ferc.gov/ eventcalendar/Files/ 20120420161518-AD12-10-000.pdf.
31. Kumar A, Srivastava SC, Singh SN. A zonal congestion management approach using real and reactive power rescheduling. *IEEE Transactions on Power Systems* 2004; **19**:554–562.
32. Moradzadeh B, Tomsovic K. Mixed integer programming-based reconfiguration of a distribution system with battery storage. *North American Power Symposium* 2012; **1–6**.
33. M.B. Liu, C.A. Canizares, and W. Huang, Reactive power and voltage control in distribution systems with limited switching operations *IEEE Trans. Power Syst.*, vol. 24, no. 2, pp. 889–899, May. 2009.
34. Soroudi A, Ehsan M. Imperialist competition algorithm for distributed generation connections. *IET Gener. Transm. Dis.* 2012; **6**:21–29.
35. Chen C, Duan S, Cai T, Liu B, Hu G. Smart energy management system for optimal microgrid economic operation. *IET Renew. Power Gen.* 2011; **5**:258–267.
36. Logenthiran T, Srinivasan D, Shun TZ. Demand side management in smart grid using heuristic optimization. *IEEE Transactions on Smart Grid* 2012; **3**:1244–1252.
37. Goldberg DE. *Genetic Algorithms in Search, Optimization and Machine Learning*. Addison-Wesley Publishing Company, Pearson Education (US), 1989; 65–90.
38. Wong S, Bhattacharya K, Fuller JD. Electric power distribution system design and planning in a deregulated environment. *IET Gener. Transm. Dis.* 2009; **3**:1061–1078.
39. Sousa T, Morais H, Vale Z, Faria P, Soares J. Intelligent energy resource management considering

vehicle-to-grid: a simulated annealing approach. *IEEE Transactions on Smart Grid* 2012; **3**:535–542.

40. Sousa T, Morais H, Soares J, Vale Z. Day-ahead resource scheduling in smart grids considering vehicle-to-grid and network constraints. *Applied Energy* 2012; **96**:183–193.
41. Baran ME, Wu F. Network reconfiguration in distribution system for loss reduction and load balancing. *IEEE Trans. Power Del.* 1989; **4**:1401–1407.
42. Ziari I, Ledwich G, Ghosh A, Platt G. Optimal distribution network reinforcement considering load growth, line loss, and reliability. *IEEE Transactions on Power Systems* 2013; **28**:587–597.
43. Recloser based automation solutions for smart grid up to 40.5 KV, Available: http://www.tavrida.eu /?action=tavrida.page&menuid=79
44. Outdoor medium voltage automatic circuit reclosers. Available: http://www.alibaba.com/ product-detail/33KV-automatic-circuit-recloser ACR_1673941121.html.
45. New York independent system operator. Available: http://www. nyiso.com, accessed July 2013.